

UCSF

UC San Francisco Previously Published Works

Title

Novel Brain Arteriovenous Malformation Mouse Models for Type 1 Hereditary Hemorrhagic Telangiectasia

Permalink

<https://escholarship.org/uc/item/9t39f2n7>

Journal

PLOS ONE, 9(2)

ISSN

1932-6203

Authors

Choi, Eun-Jung
Chen, Wanqiu
Jun, Kristine
[et al.](#)

Publication Date

2014

DOI

10.1371/journal.pone.0088511

Peer reviewed

Novel Brain Arteriovenous Malformation Mouse Models for Type 1 Hereditary Hemorrhagic Telangiectasia

Eun-Jung Choi¹, Wanqiu Chen¹, Kristine Jun¹, Helen M. Arthur², William L. Young^{1,3,4}, Hua Su^{1*}

1 Center for Cerebrovascular Research, Department of Anesthesia and Perioperative Care, University of California San Francisco, San Francisco, California, United States of America, **2** Institute of Genetic Medicine, International Centre for Life, Newcastle University, Newcastle, United Kingdom, **3** Department of Neurological Surgery, University of California San Francisco, San Francisco, California, United States of America, **4** Department of Neurology, University of California San Francisco, San Francisco, California, United States of America

Abstract

Endoglin (ENG) is a causative gene of type 1 hereditary hemorrhagic telangiectasia (HHT1). HHT1 patients have a higher prevalence of brain arteriovenous malformation (AVM) than the general population and patients with other HHT subtypes. The pathogenesis of brain AVM in HHT1 patients is currently unknown and no specific medical therapy is available to treat patients. Proper animal models are crucial for identifying the underlying mechanisms for brain AVM development and for testing new therapies. However, creating HHT1 brain AVM models has been quite challenging because of difficulties related to deleting *Eng*-floxed sequence in *Eng*^{2fl/2fl} mice. To create an HHT1 brain AVM mouse model, we used several Cre transgenic mouse lines to delete *Eng* in different cell-types in *Eng*^{2fl/2fl} mice: *R26CreER* (all cell types after tamoxifen treatment), *SM22 α -Cre* (smooth muscle and endothelial cell) and *LysM-Cre* (lysosome M-positive macrophage). An adenoviral vector expressing vascular endothelial growth factor (AAV-VEGF) was injected into the brain to induce focal angiogenesis. We found that *SM22 α -Cre*-mediated *Eng* deletion in the embryo caused AVMs in the postnatal brain, spinal cord, and intestines. Induction of *Eng* deletion in adult mice using *R26CreER* plus local VEGF stimulation induced the brain AVM phenotype. In both models, *Eng*-null endothelial cells were detected in the brain AVM lesions, and formed mosaicism with wildtype endothelial cells. However, *LysM-Cre*-mediated *Eng* deletion in the embryo did not cause AVM in the postnatal brain even after VEGF stimulation. In this study, we report two novel HHT1 brain AVM models that mimic many phenotypes of human brain AVM and can thus be used for studying brain AVM pathogenesis and testing new therapies. Further, our data indicate that macrophage *Eng* deletion is insufficient and that endothelial *Eng* homozygous deletion is required for HHT1 brain AVM development.

Citation: Choi E-J, Chen W, Jun K, Arthur HM, Young WL, et al. (2014) Novel Brain Arteriovenous Malformation Mouse Models for Type 1 Hereditary Hemorrhagic Telangiectasia. PLoS ONE 9(2): e88511. doi:10.1371/journal.pone.0088511

Editor: Klaus Brusgaard, Odense University hospital, Denmark

Received: October 2, 2013; **Accepted:** January 8, 2014; **Published:** February 10, 2014

Copyright: © 2014 Choi et al. This is an open-access article distributed under the terms of the Creative Commons Attribution License, which permits unrestricted use, distribution, and reproduction in any medium, provided the original author and source are credited.

Funding: This research was supported by grants to HS from the National Institutes of Health (R01NS027713 and P01NS044155), and from the Leslie Munzer Foundation; additional support was provided by a grant to WLY from the Michael Ryan Zodda Foundation. The funders had no role in study design, data collection and analysis, decision to publish, or preparation of the manuscript.

Competing Interests: The authors have declared that no competing interests exist.

* E-mail: hua.su@ucsf.edu

Introduction

Hereditary hemorrhagic telangiectasia (HHT), also known as Osler-Weber-Rendu (OWR) syndrome, is the first identified human disease caused by defects in a transforming growth factor- β (TGF- β) superfamily receptor [1]. It is an autosomal dominant genetic disorder of the blood vessels that manifests epistaxis, mucocutaneous telangiectases, and arteriovenous malformations (AVMs) in multiple organs including the brain, lung, liver, gastrointestinal tract, and spinal cord [2]. Most of HHT cases are categorized into either HHT type 1 (HHT1) caused by mutations in endoglin (*ENG*), a TGF- β type III auxiliary receptor mapped on chromosome 9 [1], or HHT type 2 (HHT2) caused by mutations in activin receptor-like kinase 1 (*ACVRL1*; *ALK1*), a TGF- β type I serine-threonine kinase receptor located in chromosome 12 [3]. The prevalence of brain AVM in HHT1 patients is 1000-fold higher, and in HHT2, 100-fold higher, than the prevalence in the general population (10/100,000) [4].

Brain AVM is a tangle of abnormal vessels called nidus, where blood directly shunts from arteries into veins without passing the

capillary bed. These abnormal vessels tend to rupture, causing spontaneous and recurrent hemorrhages in the brain, especially in children and young adults [5]. The life-threatening intracranial hemorrhage (ICH) risk rate in HHT patients ranges from 1.4% to 2% per year [6]. Currently available therapies, including microsurgery, embolization and/or radiosurgery, are invasive and associated with considerable side effects [7,8]. No specific medical therapy is available for brain AVM patients.

The pathogenesis of HHT brain AVMs remains largely unknown. A reliable animal model is crucial for studying disease mechanisms and testing new therapies. We and others have reported HHT2 developmental [9,10] and adult onset brain AVM phenotypes [11] in *Alk1*-conditional knockout mice. No compelling HHT1 brain AVM model has been reported.

We have previously shown that microscopic (capillary level) cerebrovascular dysplasia can be induced by focal VEGF stimulation in adult *Eng*-haploinsufficient (*Eng*^{+/-}) mice [12]. Arteriovenous (A-V) shunting has not been identified in this model. To create an adult onset HHT1 brain AVM model that closely resembles human disease, we attempted using the same

strategy that we previously used to develop an HHT2 model: stereotactic injection of a cre-expressing adenoviral vector (Ad-Cre) [11] and an adeno-associated viral vector expressing vascular endothelial growth factor (AAV-VEGF). However, Ad-Cre-mediated *Eng* deletion in the brain of *Eng*^{2fl/2fl} mice was very limited, in only about 1% of cells [13]. Only a few macroscopic level dysplasia vessels developed. The objective of this study is to establish HHT1 brain AVM mouse models that closely mimic the human brain AVM phenotype. The secondary objective is to explore *Eng* deletion in which cell-type is required for brain AVM development.

We used several cre transgenic lines in this study to achieve effective *Eng* deletion in *Eng*^{2fl/2fl} mice. Striking brain AVM phenotypes have been developed in *Eng*^{2fl/2fl};SM22 α -Cre mice spontaneously and *Eng*^{2fl/2fl};R26CreER mice after tamoxifen (TM) treatment and focal VEGF stimulation. The AVM phenotypes in these models mimic many characteristics of human brain AVM, such as arteriovenous shunting, macrophage infiltration, and microhemorrhage. Although effective *Eng* deletion in macrophages was achieved, brain AVMs did not develop in *Eng*^{2fl/2fl};LysM-Cre mice after VEGF stimulation, indicating that deletion of *Eng* in macrophages is not sufficient to cause AVM formation. However, homozygous *Eng* deletion in endothelial cells might be required for brain AVM development, because *Eng*-null endothelial cells were detected in AVM vessels in both *Eng*^{2fl/2fl};SM22 α Cre and *Eng*^{2fl/2fl};R26CreER mice.

Materials and Methods

Ethics statement

The protocol and experimental procedures for using laboratory animals were approved by the Institutional Animal Care and Use Committee (IACUC) of the University of California, San Francisco (UCSF). Animal husbandry was provided by the staff of the IACUC of UCSF, under the guidance of supervisors who are certified Animal Technologists, and by the staff of the Animal Core Facility. Veterinary care was provided by IACUC faculty members and veterinary residents located on the San Francisco General Hospital campus. All mice were housed in a pathogen-free area in 421 \times 316 cm² cages with 12 hours light/dark cycle.

Animals

To establish various *Eng*-conditional knockout mouse lines, *Eng*^{2fl/2fl} (exons 5 and 6 flanked by loxP sites) [14] mice were crossbred with R26CreER, SM22 α -Cre, and LysM-Cre [15] mice (Jackson Laboratory, Bar Harbor, Maine).

Viral vector stereotactic injection and TM intraperitoneal administration

AAV-VEGF or AAV-LacZ (vector control) [16] was injected into the brain of 8 to 10-week-old *Eng*^{2fl/2fl};R26CreER and *Eng*^{2fl/2fl};LysM-Cre mice (6 mice per group), as previously described [17]. Briefly, mice were anesthetized with isoflurane inhalation and positioned in a stereotactic frame (David Kopf Instruments). A hole was made in the pericranium, 1 mm posterior to the coronal suture and 2 mm lateral to the sagittal suture. AAV-VEGF viral suspension (2×10^9 genome copies) was stereotactically injected into the right basal ganglia at 3 mm in depth from the cortex. TM dissolved in corn oil (2.5 mg/25 g of body weight; Sigma-Aldrich) was injected intraperitoneally [9] to *Eng*^{2fl/2fl};R26CreER mice for 3 consecutive days starting from the day of viral vector injection (Figure S1A).

Systemic latex vascular casting

Systemic latex dye perfusion, described previously [9,11], was performed by injecting blue latex dye (Connecticut Valley Biological Supply) into the left ventricle of the heart. Brain, lung, kidney, liver, intestine and ear were collected and fixed in 4% paraformaldehyde overnight and imaged under a light microscope. Organs were then sequentially dehydrated in a methanol series, cleared in organic solvent (benzyl benzoate/benzyl alcohol, 1:1; Sigma-Aldrich), and imaged again under a light microscope.

Dysplasia index quantification

Two 20 μ m-thick coronal brain sections per animal, 0.5 mm rostral and 0.5 mm caudal to the virus injection site, were stained with lectin (1:200; Vector Laboratories). Three areas (to the right and left of and below the injection site) within the angiogenic region of each section were imaged under the 20X microscopic objective lens for quantification. Dysplasia index (number of vessels larger than 15 μ m in diameter per 100 blood vessels) was calculated by three blinded investigators using NIH Image 1.63 software as previously described [11–13,17].

Immunohistochemistry

Mice were anesthetized with isoflurane inhalation and perfused with heparin/PBS to remove blood. Brain samples were harvested and frozen in dry ice, then sectioned into 20 μ m sections. The location of AVM lesions was first identified through staining 1 of every 10 sections with lectin (1:200; Vector Laboratories). Sections containing dysplastic vessels were then co-stained with primary antibodies against CD31 (1:50; Abcam) and CD68 (1:50; AbD Serotec). Each protein was subsequently visualized using fluorescently labeled secondary antibodies: Alexa Fluor 488 goat anti-rabbit IgG (1:500; Invitrogen) for CD31, and Alexa Fluor 594 goat anti-rat IgG (1:500; Invitrogen) for CD68. ENG expression was identified by an antibody against ENG/CD105 (1:50; BD Pharmingen) and visualized by a biotin-conjugated secondary antibody (anti-rat IgG, 1:500; Vector Laboratories), using the standard ABC method (Vector immunodetection kit; Vector Laboratories). Prussian blue staining was performed according to the protocol provided by the company (Iron Stain Kit; Sigma-Aldrich).

Monocyte/macrophage isolation and culture

Monocytes/macrophages were isolated and cultured as previously described [17]. Briefly, bone marrow was collected from tibias and femurs of 8-week-old *Eng*^{2fl/2fl} and *Eng*^{2fl/2fl};LysM-Cre mice and cultured in a macrophage-enriched medium containing mouse macrophage-colony stimulating factor (M-CSF, 7.5 ng/ml; Akron Biotech) and 10% fetal bovine serum (FBS) for 7 days.

Real-time quantitative genomic DNA PCR analysis

DNA was isolated from the brain of 3 control *Eng*^{2fl/2fl} and 3 TM-treated *Eng*^{2fl/2fl};R26-CreER mice, and macrophages were isolated from 3 *Eng*^{2fl/2fl} and 3 *Eng*^{2fl/2fl};LysM-Cre mice. Recombination of the *Eng* 2fl (floxed) allele was quantified using Mx3000P QPCR System (Agilent Technologies). The gene deletion efficiency was calculated as the amount of *Eng* 2fl in experimental samples/*Eng*2fl levels in controls times 100. The primers used for real-time qPCR are listed in Table S1.

Statistical analysis

Data are represented as mean \pm SD. Student's t-test was used to determine a statistical significance between groups. A p value of <0.05 was considered statistically significant. The survival curve

of $Eng^{2fl/2fl};SM22\alpha$ -Cre mice was made and the difference between male and female mice was analyzed using Prism 6 software.

Results

Developmental onset of brain AVM in $Eng^{2fl/2fl};SM22\alpha$ -Cre mice

The $SM22\alpha$ -Cre transgenic mouse induced target gene deletion in vascular smooth muscle cells during the embryonic developmental stage. In addition to vascular smooth muscle cells, $SM22\alpha$ -Cre transgene has been shown to mediate gene deletion in endothelial cells and some other cell-types [10]. To test if $SM22\alpha$ -Cre-mediated Eng deletion in the embryo leads to postnatal brain AVM, we crossbred $Eng^{2fl/2fl}$ mice with $SM22\alpha$ -Cre mice. Three different mouse groups were obtained: $Eng^{2fl/2fl}$, $Eng^{+/-};SM22\alpha$ -Cre, and $Eng^{2fl/2fl};SM22\alpha$ -Cre. The AVM phenotype (greatly enlarged and tortuous vessels) was detected in the brain of 90% (18 out of 20) of 5-week-old $Eng^{2fl/2fl};SM22\alpha$ -Cre mice that had Eng homozygous deletion in Cre-expressing cells (Figure 1C and 1F). More than 80% of the mice had one lesion, while the remaining 20% had 2–3 lesions. No AVM phenotype was observed in the brain of $Eng^{2fl/2fl}$ littermates that did not have Cre transgene (wildtype) (Figure 1A and 1D) and $Eng^{+/-};SM22\alpha$ -Cre mice that had one Eng allele deletion (heterozygous, Figure 1B and 1E). AVMs were also found in the spinal cord (Figure S2C) and intestine (Figure S2F) of $Eng^{2fl/2fl};SM22\alpha$ -Cre mice, but not in $Eng^{2fl/2fl}$ and $Eng^{+/-};SM22\alpha$ -Cre mice (Figure S2A, S2B, S2D, and S2E). The brain lesions varied in size, location (Figure S3A and S3B), and number. There was latex dye found in the veins (indicative of A–V shunting), and hemorrhage in some brain and spinal cord lesions (Figure S3C and S3D). More than 50% of the $Eng^{2fl/2fl};SM22\alpha$ -Cre mice died before 6 weeks of age (Figure 1G). The survival rates were similar in males and females ($P = 0.47$).

Adult onset brain AVM in $Eng^{2fl/2fl};R26CreER$ mice after TM treatment and focal angiogenic stimulation

To induce the adult onset HHT1 brain AVM phenotype, we utilized the $R26CreER$ transgenic mouse in which Cre expression is activated by TM treatment [9] to conditionally delete the Eng gene. Eng deletion in adult $Eng^{2fl/2fl};R26CreER$ mice was induced by intraperitoneal injection of TM for 3 consecutive days (Figure S1A). About 60% of Eng -floxed allele was deleted in the brain (Figure S1B). Eng deletion alone did not affect the established vasculature in the adult brain (Figure 2A). However, the AVM phenotype developed in AAV-VEGF-induced brain angiogenic foci 8 weeks after induction of Eng deletion and angiogenesis (Figure 2B). Notably, the lesions mimicked the human brain AVM nidus (Figure 2C) and consisted of markedly enlarged vessels (Figure 2D). More enlarged vessels were detected in AAV-VEGF-injected sites (angiogenic foci) than in AAV-LacZ-injected (control vector) sites in the brain of TM-treated $Eng^{2fl/2fl};R26CreER$ mice (dysplasia index: 2.9 ± 0.5 versus 0.05 ± 0.05 , $p < 0.05$, Figure 2E). Since the brain AVMs in $Eng^{2fl/2fl};R26CreER$ were induced by VEGF, the lesions were thus always located at the AAV-VEGF injection sites. Further, the AVM phenotype was also detected around the ear-tag wound of all TM treated $Eng^{2fl/2fl};R26CreER$ mice (Figure S4A). No AVM phenotype was found in the contralateral uninjured ear (data not shown) and the intestine (Figure S4B). Taken together, global conditional Eng deletion in adult mice resulted in de novo AVMs in the brain angiogenic foci and around the skin wound.

No AVM found in $Eng^{2fl/2fl};LysMCre$ mice

We have previously shown that bone marrow-derived macrophages home to the brain angiogenic foci [18]. $Eng^{+/-}$ mice and WT mice transplanted with $Eng^{+/-}$ bone marrow developed a similar degree of dysplasia after VEGF stimulation [17]. These data suggest that bone marrow-derived macrophages may play a role in brain AVM development. To test if Eng deletion in macrophages is sufficient to induce brain AVMs, we utilized the $LysM$ -Cre mouse [15] that specifically mediates target gene recombination in lysozyme M-positive macrophages. $Eng^{2fl/2fl};LysM$ -Cre mice are born with the expected Mendelian ratio and develop normally into the adult stage. Injection of AAV-VEGF into the basal ganglia of 8 to 10-week-old $Eng^{2fl/2fl};LysM$ -Cre mice did not induce AVM phenotype in the brain (Figure 3). Similarly, no AVM phenotype was observed around the ear wound (Figure S4C) and intestine (Figure S4D). Real-time genomic DNA qPCR analysis confirmed that more than 90% Eng was deleted in macrophages of $Eng^{2fl/2fl};LysM$ -Cre mice (Figure S5), indicating that the lack of AVM phenotype was not due to inefficient gene deletion. Thus, these data suggest that Eng deletion in lysozyme M-positive macrophages alone was not sufficient to initiate AVM formation.

Eng -null endothelial cells detected in brain AVM vessels

Dilated and dysmorphic (dysplasia) vessels were found in lectin-stained brain sections of 5-week-old $Eng^{2fl/2fl};SM22\alpha$ -Cre mice (Figure 4A) and around the brain angiogenic region of TM-treated adult $Eng^{2fl/2fl};R26CreER$ mice (Figure 4B), but not in the brain angiogenic region of adult $Eng^{2fl/2fl};LysM$ -Cre mice (Figure 4C). Endothelial ENG expression was greatly reduced in the lesions of brain sections from $Eng^{2fl/2fl};SM22\alpha$ -Cre and $Eng^{2fl/2fl};R26CreER$ mice (Figure 4D and 4E). Endothelial ENG expression in the angiogenic foci of $Eng^{2fl/2fl};LysM$ -Cre mice did not change (Figure 4F and 4I). Notably, ENG-null endothelial cells were found in large dysplastic vessels in cerebral lesions in both $Eng^{2fl/2fl};SM22\alpha$ -Cre (Figure 4G) and $Eng^{2fl/2fl};R26CreER$ (Fig. 5H) mice. Further, similar to the phenotype of the $Alk1$ -deficient model (HHT2 model) [19] and human unruptured brain AVMs [20,21], macrophages and microhemorrhage were observed around dysplastic vessels in the brain of $Eng^{2fl/2fl};SM22\alpha$ -Cre and $Eng^{2fl/2fl};R26CreER$ mice (Figure 5). Thus, all of the evidence indicates that homozygous deletion of Eng in endothelial cells is necessary for the development of macroscopic AVM-like vessels with arteriovenous (A–V) shunts in the mouse brain.

Discussion

In this study, we established two novel HHT1 brain AVM mouse models: one, developmental onset, and the other, adult onset. These models are better suited for mechanistic studies and new drug tests than the existing HHT brain AVM models we and others have developed [9–12]. We have also shown that endothelial homozygous Eng deletion is required for the development of the HHT1 brain AVM phenotype, whereas deletion of Eng in macrophages is insufficient.

As a model for investigating AVM pathogenesis and testing novel therapies, our HHT1 developmental model created in $Eng^{2fl/2fl};SM22\alpha$ -Cre mice has some advantages compared to the two HHT2 developmental brain AVM models developed in $Alk1^{2fl/2fl};L1Cre$ mice [9] and $Alk1^{2fl/2fl};SM22\alpha$ -Cre mice [10]. The $Alk1^{2fl/2fl};L1Cre$ mice died at postnatal day 5 due to massive intracranial hemorrhage [9]. More than 50% of $Alk1^{2fl/2fl};SM22\alpha$ -Cre mice died before 2 weeks of age [10]. Such a short lifespan limits their use in testing new therapies. In contrast, we did not

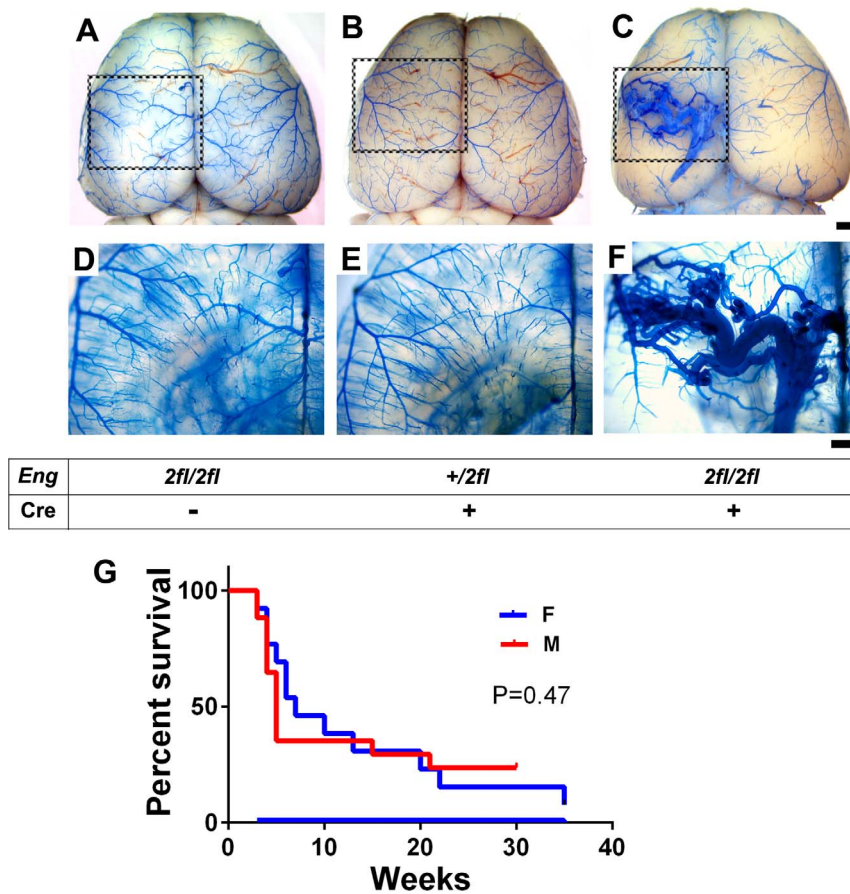


Figure 1. Developmental onset AVM in the postnatal brain of $Eng^{2fl/2fl};SM22\alpha-Cre$ mice. Representative images of latex dye casting show the cerebrovasculature in the brain of 5-week-old (A) $Eng^{2fl/2fl}$, (B) $Eng^{+2fl};SM22\alpha-Cre$, and (C) $Eng^{2fl/2fl};SM22\alpha-Cre$ mice. D–F: Enlarged images of dotted boxes shown in A–C after the brain tissue was cleared in organic solvent. The latex-perfused vasculature inside the brain can be observed. Tangled and dilated vessels were detected only in the brain of $Eng^{2fl/2fl};SM22\alpha-Cre$ mice. Scale bars: 1 mm in A–C and 500 μ m in D–F. G: Survival curve of $Eng^{2fl/2fl};SM22\alpha-Cre$ mice. There was no difference between male (M) and female (F) mice ($P=0.47$). doi:10.1371/journal.pone.0088511.g001

observe any lethality in our $Eng^{2fl/2fl};SM22\alpha-Cre$ model until postnatal week 3. About 30% of the mice died between 3 and 6 weeks due to cerebral and/or gastrointestinal hemorrhage. The penetrance of the brain AVM phenotype was about 90% at 5 weeks of age. Further, there is no other manipulation, such as angiogenic stimulation, needed to initiate brain AVM development in addition to gene deletion. Thus, brain AVM initiation and progression in $Eng^{2fl/2fl};SM22\alpha-Cre$ mice more closely resemble spontaneously developed human brain AVM, making this model more suitable for studying brain AVM pathogenesis and testing new therapies. Since the lesion size, location, and number in this model are highly variable, identifying the location of the AVM lesion and quantifying the dysplasia index by tissue section would be time consuming and challenging. However, the AVM lesions were only detected in $Eng^{2fl/2fl};SM22\alpha-Cre$ mice, and not in $Eng^{2fl/2fl}$ or $Eng^{+2fl};SM22\alpha-Cre$ mice (Figure 1). We recorded the presence of large AVMs in a whole-mount brain preparation following latex casting in 90% of $Eng^{2fl/2fl};SM22\alpha-Cre$ mice. This method detected lesions with A–V shunts (latex dye presented in the veins). More than 80% of the mice had one lesion, and the remaining 20%, 2–3 lesions. Thus, comparing the number of mice with lesions in the treated and control groups could be used to evaluate the therapeutic efficacy of new test drugs. In addition, since $Eng^{2fl/2fl};SM22\alpha-Cre$ mice died at various times (Figure 1G),

analysis of the mortality rate could be another means of evaluating a test drug's effectiveness. More detailed quantification would be extremely time consuming due to the non-specific location of the lesions, which is a limitation of the $Eng^{2fl/2fl};SM22\alpha-Cre$ model.

The capillary level dysplasia in the brain of $Eng^{+/-}$ mice described previously does not closely resemble the human brain AVM phenotype [12]. The major drawback of our published adult onset brain AVM model is that a Cre-expressing adenoviral vector was used to induce focal *Alk1* deletion [11]. Because the adenoviral vector induces potent local inflammation [22], it limits the use of this model to the study of the role of inflammation in brain AVM phenotype development and progression. We have overcome this limitation in the present model by using the *R26CreER* transgene to achieve conditional *Eng* deletion. Unlike $Alk1^{2fl/2fl};R26CreER$ mice that exhibited 100% lethality 2 to 3 weeks after TM-induced gene deletion [9], $Eng^{2fl/2fl};R26CreER$ mice treated with our selected TM dose survived more than 2 months after the induction of *Eng* deletion. After intra-brain injection of AAV-VEGF, $Eng^{2fl/2fl};R26CreER$ mice developed the phenotype resembling human brain AVM. AAV causes fewer host inflammatory and immune responses than adenoviral vectors [22]. Therefore, this is a better model for studying the role of inflammation in brain AVM pathogenesis than the model induced by Ad-Cre/AAV-VEGF-mediated focal *Alk1*-deletion and angiogenesis [11,19].

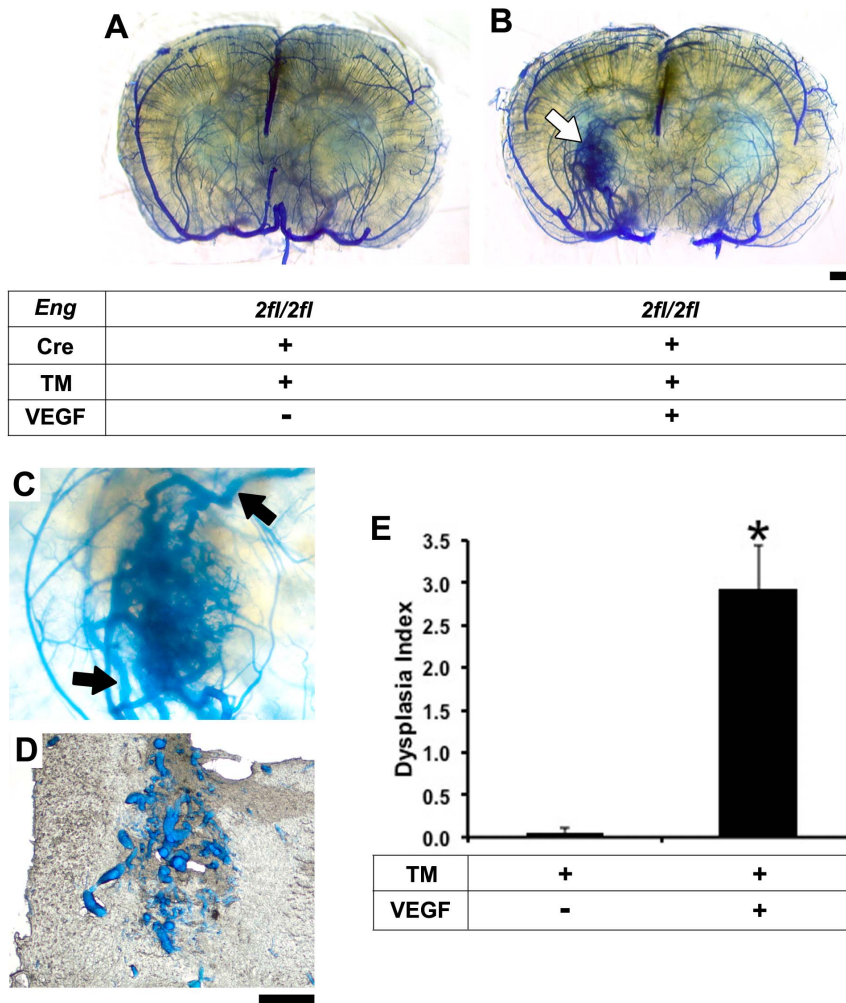


Figure 2. Adult onset brain AVM in *Eng*^{2fl/2fl};R26CreER mice after TM and VEGF treatment. A: Coronal view of latex-perfused adult *Eng*^{2fl/2fl};R26CreER brain showing no AVM phenotype 8 weeks after TM treatment. B: AVM phenotype (white arrow) developed in the brain of *Eng*^{2fl/2fl};R26CreER mice 8 weeks after intrabrain injection of AAV-VEGF and intraperitoneal injection of TM. C: An enlarged image of the AVM lesion. Latex-perfused veins are clearly shown at the top and bottom of the lesion (black arrows). D: Enlarged vessels observed in a 50 µm frozen section that cuts through the AVM lesion shown in C. E: Quantification of dysplasia index. Data: mean ± SD. *: *p* < 0.05. n = 6 per group. Scale bars: 1 mm in A and B and 500 µm in C and D.

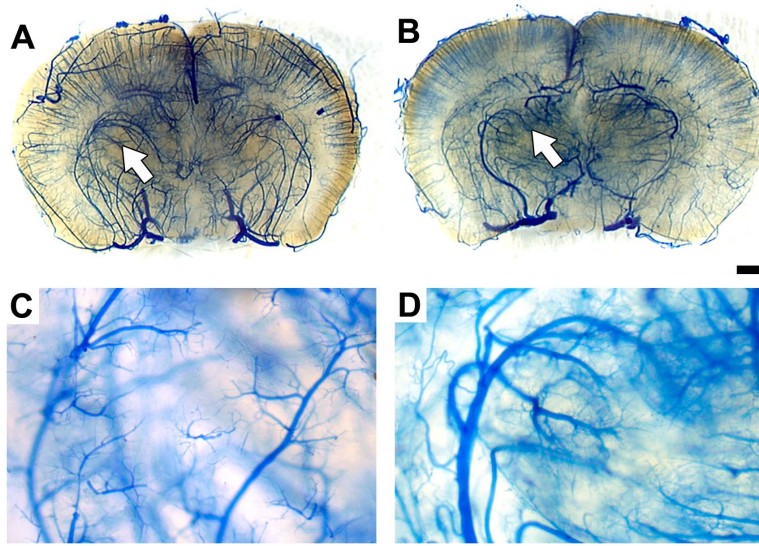
doi:10.1371/journal.pone.0088511.g002

We detected AVM only in the intestines of *Eng*^{2fl/2fl};SM22α-Cre mice, but not in *Eng*^{2fl/2fl};R26CreER mice. Interestingly, adult *Alk1*^{2fl/2fl};R26CreER mice developed AVMs in their lungs and intestines after TM treatment [9]. Additionally, *Eng*^{2fl/2fl};R26CreER mice survived 2 months after TM treatment, whereas all *Alk1*^{2fl/2fl};R26CreER mice died within 2 to 3 weeks after TM. We hypothesize that ineffective gene deletion in *Eng*^{2fl/2fl};R26CreER was responsible for some of the phenotypic difference between *Eng*^{2fl/2fl};R26CreER and *Alk1*^{2fl/2fl};R26CreER. We found in our previous study that stereotactic injection of the same dose of Ad-Cre resulted in 16% *Alk1* deletion in the brain of *Alk1*^{2fl/2fl} mice and less than 1% *Eng* deletion in *Eng*^{2fl/2fl} mice [13]. In a future study, we will use a more powerful gene deletion system to test this hypothesis.

The prevailing view regarding AVM manifestation in HHT is that it is caused by haploinsufficiency of one of its causative genes. However, *ENG* haploinsufficiency in endothelial cells in human HHT lesions appears to be insufficient for AVM development [23]. We found that *Eng* homozygous deletion in endothelial cells seems to be required for brain AVM formation. Both SM22α-Cre

and R26CreER mediate recombination of loxP sites in endothelial cells [9,10]. The fact that the brain AVM phenotype developed only in *Eng*^{2fl/2fl};SM22α-Cre and *Eng*^{2fl/2fl};R26CreER mice, but not in *Eng*^{+/2fl};SM22α-Cre and *Eng*^{+/2fl};R26CreER mice, suggests that *Eng* homozygous deletion is necessary. These data are consistent with our previous findings that: (1) only capillary level (microscopic level) vascular dysplasia developed in the brain of adult *Eng*^{+/−} and *Alk1*^{+/−} mice after intra-brain injection of AAV-VEGF [12]; and (2) *Eng* homozygous deletion of ~1% endothelial cells in the adult mouse brain was sufficient to induce the macroscopic level of cerebrovascular dysplasia phenotype [13]. Hence, loss of function of the normal allele in the endothelium of HHT patients might be necessary for AVM formation. Many factors contributing to the inactivation or downregulation of the normal allele's function have been suggested, such as focal second-hit somatic mutations, shedding of ENG from endothelial cells during inflammation [24,25], and reduced endothelial ENG signaling due to increased levels of soluble endoglin (sENG) [26].

In addition, recent studies indicate that bone marrow-derived cells play a crucial role in tissue repair and angiogenesis



<i>Eng</i>	<i>2fl/2fl</i>	<i>2fl/2fl</i>
Cre	-	+
VEGF	+	+

Figure 3. AVM phenotype was not detected in the brain angiogenic region of *Eng*^{2fl/2fl};*LysM-Cre* mice. Representative images of the latex-casted cerebrovasculature in (A) *Eng*^{2fl/2fl} and (B) *Eng*^{2fl/2fl};*LysM-Cre* adult mice 8 weeks after focal VEGF stimulation. C and D: High magnification view of the angiogenic foci (arrows) shown in A and B. Latex was present in arteries only. No vein and enlarged and tangled vessels were detected. Scale bars: 1 mm in A and B and 500 μm in C and D. doi:10.1371/journal.pone.0088511.g003

[18,27,28]. We have shown that *Eng*^{+/-} mice and WT mice transplanted with *Eng*^{+/-} bone marrow developed a similar degree of capillary level cerebrovascular dysplasia after VEGF stimulation [17]. These data suggest that bone marrow cells are involved in

brain AVM pathogenesis. Macrophage is the major bone marrow-derived cell type detected in the brain angiogenic foci [17,18,28]. To explore the role of macrophages in brain AVM development, we used *LysM-Cre* transgenic mouse lines to delete *Eng* in

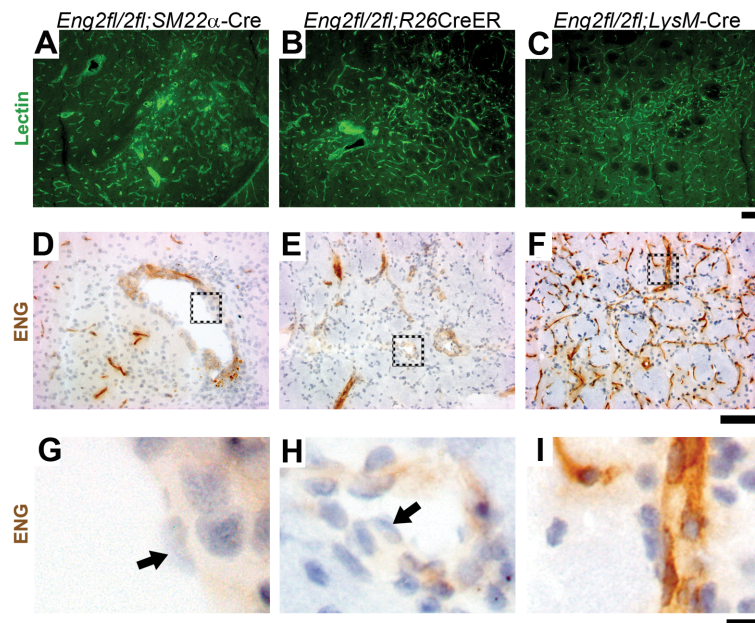


Figure 4. ENG-null endothelial cells in dysplastic vessels. Representative images of lectin-stained brain sections from (A) AVM lesion of 5-week-old *Eng*^{2fl/2fl};*SM22α-Cre*, (B) VEGF-induced angiogenic focus of TM-treated adult *Eng*^{2fl/2fl};*R26CreER*, and (C) VEGF-stimulated angiogenic focus of adult *Eng*^{2fl/2fl};*LysM-Cre* mice. ENG expression in (D) *Eng*^{2fl/2fl};*SM22α-Cre*, (E) *Eng*^{2fl/2fl};*R26CreER*, and (F) *Eng*^{2fl/2fl};*LysM-Cre* brain. G-I: Enlarged images of the dotted boxes shown in D-F. Arrows indicate ENG-negative endothelial cells. Scale bars: 100 μm in A-F and 10 μm in G-I. doi:10.1371/journal.pone.0088511.g004

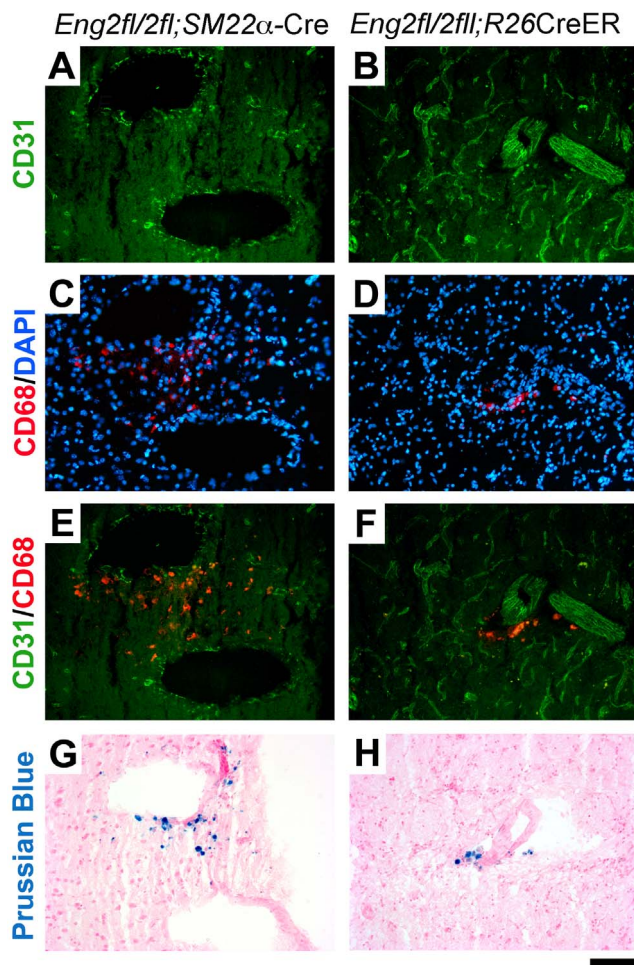


Figure 5. Macrophage infiltration and microhemorrhage in brain AVM lesions of *Eng*^{2fl/2fl};SM22 α -Cre and *Eng*^{2fl/2fl};R26CreER mice. Dysplastic vessels were present in the brain of (A) *Eng*^{2fl/2fl};SM22 α -Cre and (B) *Eng*^{2fl/2fl};R26CreER mice. Endothelial cells were visualized by immunostaining using an antibody specific to CD31 (an endothelial cell-specific marker). C and D: Macrophages were detected by immunostaining using a CD68-specific antibody. The nuclei were stained by DAPI. E and F: Macrophages localized around large dysplastic vessels. G and H: Iron deposits, an indicator of hemorrhage, identified by Prussian blue. Scale bar: 100 μ m.
doi:10.1371/journal.pone.0088511.g005

macrophages. *LysM*-Cre selectively induces gene recombination in lysozyme M-positive macrophages [15]. Mice with *LysM*-Cre-driven *Eng* deletion during the embryonic developmental stage did not develop the brain AVM phenotype even after VEGF stimulation. Therefore, deletion of *Eng* in macrophages alone is not sufficient for brain AVM formation.

However, this finding does not rule out a potential contributory role of macrophage endoglin during AVM pathogenesis. *Eng* deficiency appears to impair monocyte adhesion and migration. The homing ability of ENG-deficient HHT1 monocytes to the infarcted murine heart is impaired [27,29]. *Eng* deficiency in endothelial cells reduces leukocyte adhesion and transmigration [30] and impairs the endothelial-autonomous capacity to up-regulate SDF1 expression in response to hindlimb ischemic injury [31]. However, macrophage load is higher in unruptured human brain AVM lesions than in control vessels [20,21] and there is also high monocyte/macrophage infiltration in HHT skin lesions [32]. We previously found that a systemic reduction in endoglin levels

led to a temporal difference in macrophage responses. *Eng*^{+/-} mice had fewer CD68⁺ cells in the peri-infarct area at 3 days but more CD68⁺ cells at 60 days after permanent occlusion of a distal middle cerebral artery [33]. It appears that in the early stages of injury, there are fewer monocytes homing to the injury site. At the late stage when recovery normally occurs, more macrophages persist around abnormal vessels, potentially promoting disease progression. In addition, extravasation of blood content from dysplastic AVM vessels could also attract macrophage infiltration [19,21]. Indeed, macrophages were mostly co-localized with iron deposits around the dysplastic vessels in the two models we present in this manuscript (Figure 5). Further study will be needed to understand how macrophages enter the AVM lesion, and the correlation between macrophage load and patient outcomes.

A limitation of this study is that vascular leakage and macrophage infiltration were not quantified in these models. However, we did observe that these phenotypes were not as severe as in the *Alk1*-deficient model we previously reported [19]. The potential reasons include: (1) the vascular defect takes longer to develop in *Eng*-deficient vessels than in *Alk1*-deficient vessels; and (2) the gene deletion in our previous *Alk1* model was induced by Ad-Cre, and as a result, the inflammatory response to adenoviral vector could have resulted in increased macrophage infiltration and more severe vascular leakage [19]. In addition, ineffective gene deletion in *Eng*^{2fl/2fl};R26CreER could also be a reason for a milder phenotype. Stereotactic injection of the same dose of Ad-Cre resulted in 16% *Alk1* deletion in the brain of *Alk1*^{2fl/2fl} mice and less than 1% *Eng* deletion in *Eng*^{2fl/2fl} mice [13]. In the future, we will observe the lesion for a longer period of time, or use a more powerful cre system.

Although many advances have been made in the HHT field, the underlying molecular and cellular mechanisms for AVM formation are still unclear. Our novel mouse brain AVM models would be valuable resources for dissecting brain AVM pathogenesis. Studying more common familial brain AVM cases will help us understand unknown causes of sporadic brain AVMs. The detailed long-term natural history of these models would also allow us to understand the progression of brain AVM, paving the way towards improving patient care. Further, preclinical studies using these animals will lead to the design of a safer and more effective pharmacological therapy for HHT brain AVM patients, which may also apply to patients with sporadic brain AVM.

Supporting Information

Table S1 Primers used for real-time quantitative genomic DNA PCR analysis. Matrix metalloproteinase 9 (*Mmp9*) was used as an internal quantitative control. (DOCX)

Figure S1 Conditional *Eng* deletion in the adult mouse using the R26CreER transgenic mouse. A: Experimental design. TM was injected to *Eng*^{2fl/2fl};R26Cre-ER mice i.p. once per day for 3 consecutive days. AAV-VEGF was injected into the right basal ganglia at the time when the first dose of TM was given. Samples were collected for phenotype analysis 8 weeks after the TM and AAV-VEGF injection. B: Quantification of WT *Eng* (2fl) allele in the genomic DNA isolated from the brain 8 weeks after the first tamoxifen (TM) injection. n = 3 per group. (TIF)

Figure S2 SM22 α -Cre-driven *Eng* deletion resulted in AVMs in the postnatal spinal cord and intestine. AVM

phenotypes in the (C) spinal cord and (F) intestine of *Eng*^{2fl/2fl}; *SM22 α* -Cre mice, but not in those of control mice (A, B, D, and E). Arteries (a) and veins (v) are shown in dark and light blue, respectively, in the intestine of *Eng*^{2fl/2fl}; *SM22 α* -Cre mice. Scale bars: 1 mm.

(TIF)

Figure S3 AVMs and microhemorrhages found in the brain and spinal cord of 5-week-old *Eng*^{2fl/2fl}; *SM22 α* -Cre mice. Examples of (A) superficially and (B) deeply located brain AVMs. Hemorrhages (arrows) detected in some lesions of the (C) brain and (D) spinal cord. a: Artery. v: Vein. Scale bars: 1 mm.

(TIF)

Figure S4 *R26CreER*-mediated conditional *Eng* deletion induced de novo skin AVMs around the ear wound. A: AVM vessels around the ear wound (*) of tamoxifen-treated *Eng*^{2fl/2fl}; *R26CreER* mice. B: No arteriovenous (A–V) shunts in the intestine of *Eng*^{2fl/2fl}; *R26CreER* mice 8 weeks after tamoxifen treatment. No abnormal vascular phenotype observed around the

(C) ear wound (*) and in the (D) intestine of *Eng*^{2fl/2fl}; *LysM-Cre* mice. Scale bars: 1 mm.

(TIF)

Figure S5 *LysM-Cre* induced effective *Eng* deletion in macrophages. Relative amount of the targeted *Eng* conditional 2fl allele in *Eng*^{2fl/2fl}; *LysM-Cre* macrophages compared to that of *Eng*^{2fl/2fl} macrophages. n = 3 per group.

(TIF)

Acknowledgments

We thank Voltaire Gungab for manuscript preparation, the UCSF BAVM project members (<http://avm.ucsf.edu>) for their support, and Dr. S. Paul Oh at the University of Florida for critical review of the manuscript.

Author Contributions

Conceived and designed the experiments: EJC HS WLY. Performed the experiments: EJC WC KJ. Analyzed the data: EJC WC KJ HA HS. Contributed reagents/materials/analysis tools: HA. Wrote the paper: EJC HS. Obtained financial support: WLY HS.

References

- McAllister KA, Grogg KM, Johnson DW, Gallione CJ, Baldwin MA, et al. (1994) Endoglin, a TGF-beta binding protein of endothelial cells, is the gene for hereditary haemorrhagic telangiectasia type 1. *Nat Genet* 8: 345–351.
- Shovlin CL, Guttmacher AE, Buscarini E, Faughnan ME, Hyland RH, et al. (2000) Diagnostic criteria for hereditary hemorrhagic telangiectasia (Rendu-Osler-Weber syndrome). *Am J Med Genet* 91: 66–67.
- Johnson DW, Berg JN, Baldwin MA, Gallione CJ, Marondel I, et al. (1996) Mutations in the activin receptor-like kinase 1 gene in hereditary haemorrhagic telangiectasia type 2. *Nat Genet* 13: 189–195.
- Kim H, Marchuk DA, Pawlikowska L, Chen Y, Su H, et al. (2008) Genetic considerations relevant to intracranial hemorrhage and brain arteriovenous malformations. *Acta Neurochir Suppl* 105: 199–206.
- Kim H, Su H, Weinsheimer S, Pawlikowska L, Young WL (2011) Brain arteriovenous malformation pathogenesis: a response-to-injury paradigm. *Acta Neurochir Suppl* 111: 83–92.
- Easey AJ, Wallace GM, Hughes JM, Jackson JE, Taylor WJ, et al. (2003) Should asymptomatic patients with hereditary haemorrhagic telangiectasia (HHT) be screened for cerebral vascular malformations? Data from 22,061 years of HHT patient life. *J Neurol Neurosurg Psychiatry* 74: 743–748.
- Han PP, Ponce FA, Spetzler RF (2003) Intention-to-treat analysis of Spetzler-Martin grades IV and V arteriovenous malformations: natural history and treatment paradigm. *J Neurosurg* 98: 3–7.
- Bambakidis NC, Cockroft K, Connolly ES, Amin-Hanjani S, Morcos J, et al. (2013) Preliminary results of the ARUBA study. *Neurosurgery* 73: E379–381.
- Park SO, Wankhede M, Lee YJ, Choi EJ, Fliess N, et al. (2009) Real-time imaging of de novo arteriovenous malformation in a mouse model of hereditary hemorrhagic telangiectasia. *J Clin Invest* 119: 3487–3496.
- Milton I, Ouyang D, Allen CJ, Yanasak NE, Gossage JR, et al. (2012) Age-dependent lethality in novel transgenic mouse models of central nervous system arteriovenous malformations. *Stroke* 43: 1432–1435.
- Walker EJ, Su H, Shen F, Choi EJ, Oh SP, et al. (2011) Arteriovenous malformation in the adult mouse brain resembling the human disease. *Ann Neurol* 69: 954–962.
- Hao Q, Zhu Y, Su H, Shen F, Yang GY, et al. (2010) VEGF induces more severe cerebrovascular dysplasia in Endoglin^{+/-} than in Alk1^{+/-} mice. *Transl Stroke Res* 1: 197–201.
- Choi EJ, Walker EJ, Shen F, Oh SP, Arthur HM, et al. (2012) Minimal homozygous endothelial deletion of *Eng* with VEGF stimulation is sufficient to cause cerebrovascular dysplasia in the adult mouse. *Cerebrovasc Dis* 33: 540–547.
- Allinson KR, Carvalho RL, van den Brink S, Mummery CL, Arthur HM (2007) Generation of a floxed allele of the mouse Endoglin gene. *Genesis* 45: 391–395.
- Clausen BE, Burkhardt C, Reith W, Renkawitz R, Forster I (1999) Conditional gene targeting in macrophages and granulocytes using *LysMcre* mice. *Transgenic Res* 8: 265–277.
- Su H, Lu R, Kan YW (2000) Adeno-associated viral vector-mediated vascular endothelial growth factor gene transfer induces neovascular formation in ischemic heart. *Proc Natl Acad Sci U S A* 97: 13801–13806.
- Choi EJ, Walker EJ, Degos V, Jun K, Kuo R, et al. (2013) Endoglin deficiency in bone marrow is sufficient to cause cerebrovascular dysplasia in the adult mouse after vascular endothelial growth factor stimulation. *Stroke* 44: 795–798.
- Hao Q, Liu J, Pappu R, Su H, Rola R, et al. (2008) Contribution of bone marrow-derived cells associated with brain angiogenesis is primarily through leucocytes and macrophages. *Arterioscler Thromb Vasc Biol* 28: 2151–2157.
- Chen W, Guo Y, Walker EJ, Shen F, Jun K, et al. (2013) Reduced mural cell coverage and impaired vessel integrity after angiogenic stimulation in the *Alk1*-deficient brain. *Arterioscler Thromb Vasc Biol* 33: 305–310.
- Chen Y, Zhu W, Bollen AW, Lawton MT, Barbaro NM, et al. (2008) Evidence of inflammatory cell involvement in brain arteriovenous malformations. *Neurosurgery* 62: 1340–1349.
- Guo Y, Saunders T, Su H, Kim H, Akkoc D, et al. (2012) Silent intrasession microhemorrhage as a risk factor for brain arteriovenous malformation rupture. *Stroke* 43: 1240–1246.
- Zaiss AK, Liu Q, Bowen GP, Wong NC, Bartlett JS, et al. (2002) Differential activation of innate immune responses by adenovirus and adeno-associated virus vectors. *J Virol* 76: 4580–4590.
- Bourdeau A, Cymerman U, Paquet ME, Meschino W, McKinnon WC, et al. (2000) Endoglin expression is reduced in normal vessels but still detectable in arteriovenous malformations of patients with hereditary hemorrhagic telangiectasia type 1. *Am J Pathol* 156: 911–923.
- Li C, Guo B, Ding S, Rius C, Langa C, et al. (2003) TNF alpha down-regulates CD105 expression in vascular endothelial cells: a comparative study with TGF beta 1. *Anticancer Res* 23: 1189–1196.
- Mahmoud M, Allinson KR, Zhai Z, Oakenfull R, Ghandi P, et al. (2010) Pathogenesis of arteriovenous malformations in the absence of endoglin. *Circ Res* 106: 1425–1433.
- Chen Y, Hao Q, Kim H, Su H, Letarte M, et al. (2009) Soluble endoglin modulates aberrant cerebral vascular remodeling. *Ann Neurol* 66: 19–27.
- van Laake LW, van den Driesche S, Post S, Feijen A, Jansen MA, et al. (2006) Endoglin has a crucial role in blood cell-mediated vascular repair. *Circulation* 114: 2288–2297.
- Hao Q, Su H, Palmer D, Sun B, Gao P, et al. (2011) Bone marrow-derived cells contribute to vascular endothelial growth factor-induced angiogenesis in the adult mouse brain by supplying matrix metalloproteinase-9. *Stroke* 42: 453–458.
- Post S, Smits AM, van den Broek AJ, Sluijter JP, Hofer IE, et al. (2010) Impaired recruitment of HHT-1 mononuclear cells to the ischaemic heart is due to an altered CXCR4/CD26 balance. *Cardiovasc Res* 85: 494–502.
- Rossi E, Sanz-Rodriguez F, Eleno N, Duwell A, Blanco FJ, et al. (2013) Endothelial endoglin is involved in inflammation: role in leukocyte adhesion and transmigration. *Blood* 121: 403–415.
- Young K, Conley B, Romero D, Tweedie E, O'Neill C, et al. (2012) BMP9 regulates endoglin-dependent chemokine responses in endothelial cells. *Blood* 120: 4263–4273.
- Braverman IM, Keh A, Jacobson BS (1990) Ultrastructure and three-dimensional organization of the telangiectases of hereditary hemorrhagic telangiectasia. *J Invest Dermatol* 95: 422–427.
- Shen F, Degos V, Han Z, Choi EJ, Young WL, et al. (2013) Endoglin deficiency exacerbates ischemic brain injury (Abstract). *Stroke* 44: ATMP69.